Cell, Vol. 97, 221–231, April 16, 1999, Copyright ©1999 by Cell Press

The Interaction between N-WASP and the Arp2/3 Complex Links Cdc42-Dependent Signals to Actin Assembly

Rajat Rohatgi,*‖ Le Ma,*‖ Hiroaki Miki,‡ Marco Lopez,*† Tomas Kirchhausen,*† Tadaomi Takenawa,‡ and Marc W. Kirschner*§

*Department of Cell Biology
†The Center for Blood Research
Harvard Medical School
Boston, Massachusetts 02115
‡Department of Biochemistry
Institute of Medical Science
University of Tokyo
Tokyo 108
Japan

Summary

Although small GTP-binding proteins of the Rho family have been implicated in signaling to the actin cytoskeleton, the exact nature of the linkage has remained obscure. We describe a novel mechanism that links one Rho family member, Cdc42, to actin polymerization. N-WASP, a ubiquitously expressed Cdc42-interacting protein, is required for Cdc42-stimulated actin polymerization in *Xenopus* egg extracts. The C terminus of N-WASP binds to the Arp2/3 complex and dramatically stimulates its ability to nucleate actin polymerization. Although full-length N-WASP is less effective, its activity can be greatly enhanced by Cdc42 and phosphatidylinositol (4,5) bisphosphate. Therefore, N-WASP and the Arp2/3 complex comprise a core mechanism that directly connects signal transduction pathways to the stimulation of actin polymerization.

Introduction

The actin cytoskeleton is a dynamic filament network that is essential for cell movement, polarization, morphogenesis, and cell division (Drubin and Nelson, 1996; Mitchison and Cramer, 1996; Field et al., 1999). To engage in these complex behaviors, cells must direct actin assembly with a high degree of spatial and temporal resolution in response to extracellular signals. Over the last 10 years, extensive research using genetic, cell biological, and biochemical approaches has focused on the signal transduction pathways that link cell surface receptors to actin assembly at the plasma membrane.

In the early 1990s, members of the Rho family of small GTP-binding proteins (G proteins), including Rac, Rho, and Cdc42, were found to cause distinct morphological changes in the actin cytoskeleton upon injection into cultured cells (Ridley and Hall, 1992; Ridley et al., 1992; Nobes et al., 1995). Since then, Rho family G proteins have been shown to regulate actin-dependent processes in many different systems (Hall, 1998; Johnson, 1999). Because of their central role in signal transduction, a great deal of interest has focused on the identification of downstream pathways that link these G proteins to the actin cytoskeleton (Hall, 1998).

Progress has also been made in identifying components closer to the process of actin polymerization at the plasma membrane. Actin polymerization can be regulated by uncapping filament barbed ends (Hartwig et al., 1995), by severing filaments (Arber et al., 1998; Yang et al., 1998), or by de novo nucleation (Zigmond, 1998). The Arp2/3 complex is the best candidate to generate new barbed ends by stimulating nucleation (Bi and Zigmond, 1999; Machesky and Gould, 1999). The complex is composed of seven polypeptides and has been purified from *Acanthamoeba castellanii* (Machesky et al., 1994), *Saccharomyces cerevisiae* (Winter et al., 1997), humans (Welch et al., 1997b), and *Xenopus laevis* (Ma et al., 1998b). The Arp2/3 complex is required for actin assembly stimulated by the motile pathogen *Listeria monocytogenes* (Welch et al., 1997b), implicated in the polarized organization and motility of actin patches of yeast (Winter et al., 1997) and required for Cdc42-induced actin assembly in *Xenopus* egg extracts (Ma et al., 1998b). The complex nucleates filaments in vitro (Mullins et al., 1998) and is localized to actin-rich structures (Kelleher et al., 1995; Welch et al., 1997a; Winter et al., 1997).

Although the actin nucleation activity of the Arp2/3 complex is weak (Mullins et al., 1998), it can be stimulated by the *Listeria* protein ActA (Welch et al., 1998). This result points to the presence of analogous cellular mechanisms, presumably tied to signal transduction pathways, for regulating the complex (Beckerle, 1998). Our demonstration that the Arp2/3 complex is required for Cdc42-induced actin assembly in *Xenopus* extracts suggests that the Cdc42 signaling pathway might be such a cellular mechanism (Ma et al., 1998b). However, intermediate components between Cdc42 and Arp2/3 are clearly required because the complex does not directly bind to Cdc42, and it is not sufficient to mediate Cdc42-induced actin polymerization (Ma et al., 1998b).

Among all the Cdc42-interacting proteins identified to date, the WASP family proteins, especially WASP and N-WASP, are the best candidates for mediating the effects of Cdc42 on the actin cytoskeleton. WASP (*W*iskott-*A*ldrich *s*yndrome *p*rotein), which is only expressed in hematopoietic cells, was originally identified as a protein mutated in patients with Wiskott-Aldrich syndrome (WAS). N-WASP, which is ubiquitously expressed, shares ~50% homology with WASP (Fukuoka et al., 1997). Both proteins possess several domains: a pleckstrin homology (PH) domain that binds phosphatidylinositol (4,5) bisphosphate ($PI(4,5)P_2$), a Cdc42-binding (GBD) domain, a proline-rich region, a G-actin-binding verprolin homology (V) domain, a domain (C) with homology to the actin-depolymerizing protein cofilin, and finally a C-terminal acidic segment (A) (Figure 1A) (Miki et al., 1996). Both WASP and N-WASP induce actin polymerization when overexpressed in fibroblasts (Miki et al., 1996; Symons et al., 1996).

§To whom correspondence should be addressed (e-mail: marc@hms.harvard.edu).

‖These authors contributed equally to this work.

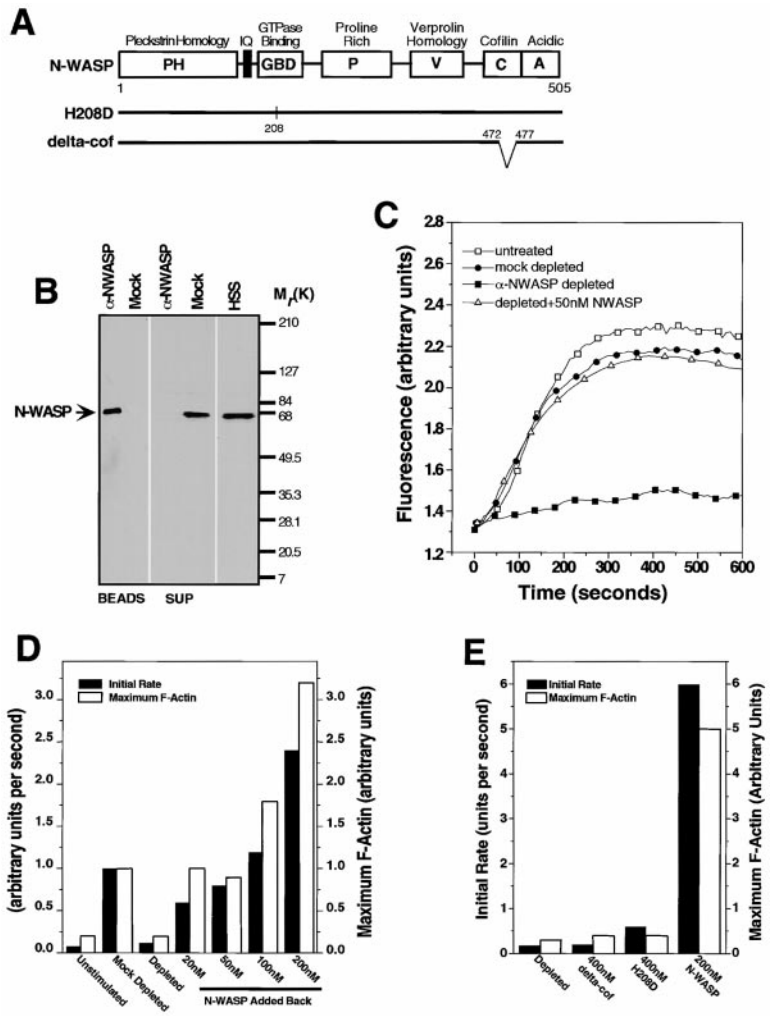

Figure 1. N-WASP Is Required for Cdc42-Induced Actin Assembly in High-Speed Supernatants of *Xenopus* Egg Extracts

(A) Schematic diagram of N-WASP showing its domain structure. Abbreviations for the domains used throughout the text are indicated inside the boxes. Numbers refer to amino acid residues. The H208D and Δcof mutants are shown below along with the sites of the mutations.

(B) Immunodepletion of N-WASP from *Xenopus* HSS. Affinity-purified α-N-WASP antibody or antibody buffer (mock) was used to immunodeplete N-WASP, and the material left in the supernatant or captured on the beads was analyzed by immunoblotting using the affinity-purified α-N-WASP antibody. 0.6% of the input material (HSS), 0.7% of the supernatant material, and 2% of the material captured on beads was loaded on the gel.

(C) Comparison of actin assembly stimulated by 250 nM GTPγS-charged GST-Cdc42 in untreated HSS, mock-depleted HSS, α-N-WASP depleted HSS, and in depleted HSS reconstituted with 50 nM recombinant N-WASP. Polymerization kinetics were monitored in the HSS using the pyrene actin assay in which fluorescence increase indicates filament formation.

(D) Comparison of actin assembly stimulated by 250 nM GTPγS-charged GST-Cdc42 in α-N-WASP depleted HSS to which the indicated concentrations of recombinant N-WASP were added. The initial rate of actin assembly and the maximum level of F-actin attained were quantitated from curves of the type shown in (C).

(E) Relative ability of wild-type N-WASP, the H208D mutant, and the Δcof mutant to restore actin assembly activity to HSS depleted of endogenous N-WASP. In all cases, actin assembly was initiated by the addition of 250 nM GTPγS-charged GST-Cdc42.

N-WASP is a particularly good candidate for mediating the effects of Cdc42 on the cytoskeleton because it can interact with a Cdc42 mutant (Y40C) that still induces filopodia but which cannot bind to a variety of other targets, including WASP (Miki et al., 1998a). In addition, dominant-negative mutations in N-WASP block Cdc42-induced filopodium formation, and wild-type N-WASP potentiates Cdc42-induced microspike formation (Miki et al., 1998a). Finally, in search for other components (Ma et al., 1998b) required for Cdc42-induced actin assembly in vitro, we found that N-WASP partially copurified with MCAP2 (*m*ediator of *C*dc42-induced *a*ctin *p*olymerization; unpublished observation).

We show here that N-WASP can activate the Arp2/3 complex to stimulate actin polymerization in vitro using purified components. This N-WASP–Arp2/3 interaction is also required for Cdc42-stimulated actin assembly in *Xenopus* egg extracts. Although full-length N-WASP is only weakly active, a C-terminal fragment confers a dramatic 30-fold acceleration of actin assembly kinetics. The activity of full-length N-WASP can be increased to levels similar to the C-terminal fragment in the presence of two putative regulators of N-WASP, Cdc42 and $PI(4,5)P_2$. Thus, the N-WASP–Arp2/3 interaction seems to be a critical link in Cdc42-dependant signaling pathways that control actin assembly.

Results

N-WASP Is Required for Cdc42-Induced Actin Polymerization in *Xenopus* Egg Extracts

We have previously described the reconstitution of Cdc42-stimulated actin assembly in high-speed supernatants from *Xenopus* egg extracts ("*Xenopus* HSS" or "*Xenopus* extract" in the rest of the text) (Ma et al., 1998a). The kinetics of actin polymerization can be monitored by supplementing the extracts with pyrene actin, a fluorescent derivative of actin that exhibits much higher fluorescence intensity when actin is assembled into filaments. Using this cell-free system, we have demonstrated a requirement for the Arp2/3 complex in Cdc42-induced actin polymerization (Ma et al., 1998b).

In order to test the requirement for N-WASP in this system, we raised a polyclonal rabbit antiserum against a full-length, recombinant rat N-WASP protein that is >90% identical to the bovine and human forms. After affinity purification, the antibody detected a single ~65 kDa band in *Xenopus* extracts on immunoblots and also immunoprecipitated it (Figure 1B). Using this affinity-purified antibody, we immunodepleted >95% of N-WASP from *Xenopus* HSS (Figure 1B). The depletion of N-WASP eliminates the ability of the extract to support Cdc42-stimulated actin polymerization (Figure 1C). The activity

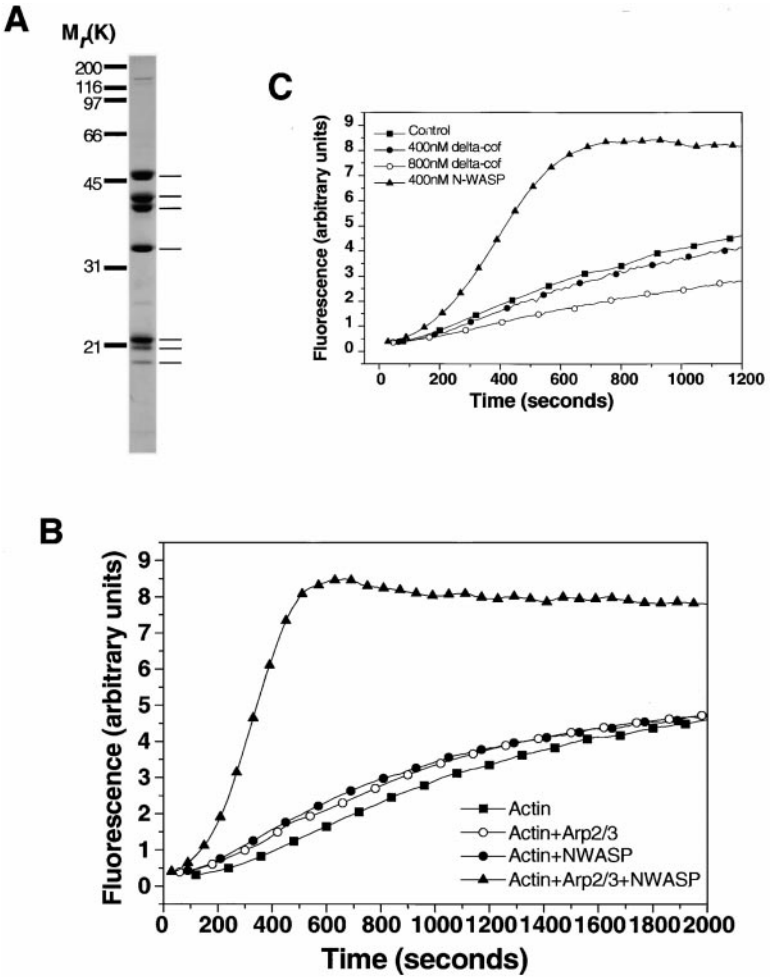

Figure 2. Full-Length N-WASP Cooperates with the Arp2/3 Complex to Accelerate Actin Polymerization In Vitro

(A) The composition of the Arp2/3 complex purified from bovine brain is shown on a 12% polyacrylamide gel stained with Gelcode Blue (Coomassie G-250). The thin, unlabeled lines on the right indicate the seven subunits of the complex. Listed in descending order of molecular weight, the subunits are Arp3, Arp2, p41-ARC, p34-ARC, p21-ARC, p20-ARC, and p16-ARC.

(B) The pyrene actin assay was used to monitor the polymerization of 2.5 μM G-actin (1.5 μM unlabeled actin + 1 μM pyrene actin) in the presence of 250 nM Arp2/3 complex alone, 400 nM N-WASP alone, or both components added together. In all the curves shown here and in the remainder of the figures, polymerization was initiated at time = 0.

(C) Comparison of the abilities of wild-type N-WASP (400 nM) and the Δcof mutant (400 nM or 800 nM) to stimulate actin polymerization in the presence of 60 nM Arp2/3 complex under conditions described in (B). The control curve depicts actin polymerization in the presence of Arp2/3 alone.

can be rescued by adding back purified recombinant N-WASP protein at approximately physiological concentrations (~20–50 nM) (Suzuki et al., 1998). Adding back increasing amounts of N-WASP leads to a dose-dependant increase both in the initial rate and in the final level of actin polymerization induced by a fixed amount of Cdc42 (Figure 1D).

The specificity of the add-back experiment was tested using two previously characterized mutants of N-WASP, H208D and Δcof (Figure 1A). H208D cannot bind to Cdc42 due to a point mutation in its Cdc42-binding domain and does not potentiate Cdc42-induced filopodia formation when introduced into cells (Miki et al., 1998a). Δcof, containing a four–amino acid deletion in the C domain of N-WASP, does not induce actin reorganization when overexpressed in Cos-7 cells and acts in a dominant-negative fashion to block Cdc42-induced filopodium formation (Miki et al., 1998a). In *Xenopus* HSS depleted of N-WASP, these mutants cannot rescue Cdc42-induced actin assembly even when added back at concentrations 20-fold above the wild-type protein (Figure 1E). These results show that regions of N-WASP implicated in interactions with both upstream regulators (Cdc42) and downstream targets are necessary for its ability to support Cdc42-induced actin assembly in *Xenopus* HSS.

Full-Length N-WASP Cooperates with the Arp2/3 Complex to Produce a Modest Acceleration of Actin Polymerization with Purified Components In Vitro

Since we had identified requirements for both N-WASP and the Arp2/3 complex in Cdc42-induced actin assembly, we wanted to determine whether N-WASP could synergize with the Arp2/3 complex to accelerate actin polymerization as observed for the ActA protein of *Listeria* (Welch et al., 1998). For these assays, we used the Arp2/3 complex purified from bovine brain extracts (Figure 2A). When we used pyrene actin fluorescence to monitor actin assembly in the presence of either pure N-WASP or pure Arp2/3 complex, the kinetics of assembly were not significantly different from those of actin alone (Figure 2B). Actin assembly kinetics demonstrate an initial lag phase, reflecting the kinetic barrier to nucleation, followed by a rapid, linear phase during which filaments elongate by monomer addition. In the presence of both Arp2/3 and N-WASP, the slope of the elongation phase is increased by ~4-fold and the lag phase is shortened, although not completely eliminated (Figure 2B). Addition of increasing amounts of N-WASP to a fixed concentration of Arp2/3 caused a dose-dependant acceleration of actin polymerization (Figure 5C).

The Δcof mutant described above does not accelerate actin assembly in the presence of the Arp2/3 complex

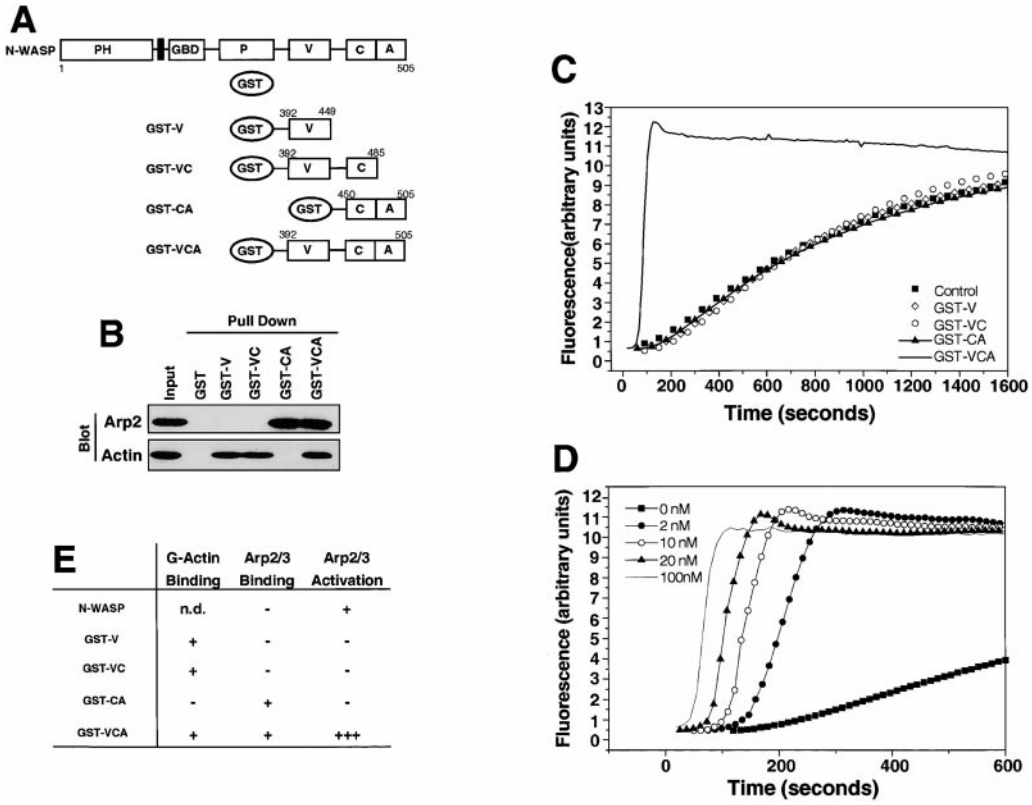

Figure 3. N-WASP Binds to and Activates the Arp2/3 Complex via Its C Terminus

(A) Schematic showing the domain structure of full-length N-WASP and the various C-terminal fragments of N-WASP constructed as GST fusion proteins. All fusion proteins are named according to the C-terminal segments (V, C, or A) of N-WASP that they contain.

(B) The GST fusion proteins shown in (A) were immobilized on glutathione-Sepharose beads and tested for their abilities to pull down either the Arp2/3 complex or G-actin from solution. The presence of the Arp2/3 complex or G-actin bound to the beads was assayed by immunoblotting with α-Arp2 or α-actin, respectively.

(C) Actin polymerization (2.5 μM actin and 60 nM Arp2/3 complex) was followed in the presence of GST-VCA (50 nM), GST-V (200 nM), GST-VC (200 nM), GST-CA (200 nM), or in the absence of any additions (control).

(D) The initial phases of actin polymerization (2.5 μM actin and 60 nM Arp2/3 complex), including the lag phase, are shown in the presence of indicated concentrations of GST-VCA.

(E) Summary of the G-actin binding, Arp2/3 binding, and Arp2/3 activation properties of full-length N-WASP and the fragments shown in (A). Binding of full-length N-WASP to Arp2/3 was determined by coimmunoprecipitation rather than GST pull down. Binding of GST-V and GST-VCA was determined by both methods.

(Figure 2C), suggesting a biochemical mechanism for its phenotypes in tissue culture cells as well as in *Xenopus* extracts (Figure 1E). Unexpectedly, the H208D mutant, which has only one point mutation in the GBD domain, does not accelerate actin assembly (data not shown), suggesting that this mutation leads to defects in functions other than just Cdc42 binding.

The C Terminus of N-WASP Strongly Accelerates Arp2/3-Mediated Actin Assembly

To define the region of N-WASP required for activity, we concentrated on a C-terminal region of N-WASP (amino acids 392–505), which contains a G-actin-binding V domain, a cofilin homology sequence (C), and an acidic segment (A) (Figures 1A and 3A). The VCA region is thought to mediate interactions of N-WASP with downstream effectors because mutations in this region abrogate its ability to induce actin rearrangements upon injection into cells and often function as dominant-negative mutations (Miki et al., 1998a). In addition, a homologous region from other WASP family proteins (Scar1/WAVE and WASP) was recently found to interact with the p21ARC subunit of the Arp2/3 complex (Machesky and Insall, 1998).

We expressed and purified GST fusion proteins containing various portions of this VCA region (diagrammed in Figure 3A) and tested their abilities to interact with the Arp2/3 complex in a GST pull-down assay. The complex bound to GST-CA and GST-VCA but not to GST, GST-V, and GST-VC (Figure 3B). As a control, the fragments were tested for binding to G-actin and, as expected, the presence of the V domain perfectly correlated with this property (Figure 3B). We conclude that the C-terminal 55 amino acids of N-WASP (450–505) are necessary and sufficient to bind to the Arp2/3 complex and that the ability to bind G-actin through the V domain is not required. We were unable to detect any interaction between full-length N-WASP and Arp2/3 by coimmunoprecipitation under conditions where the binding of GST-VCA to Arp2/3 is readily detectable (data not shown).

Since the C-terminal region of N-WASP could bind to the Arp2/3 complex and actin, we wanted to determine whether it could confer the activity of the full-length

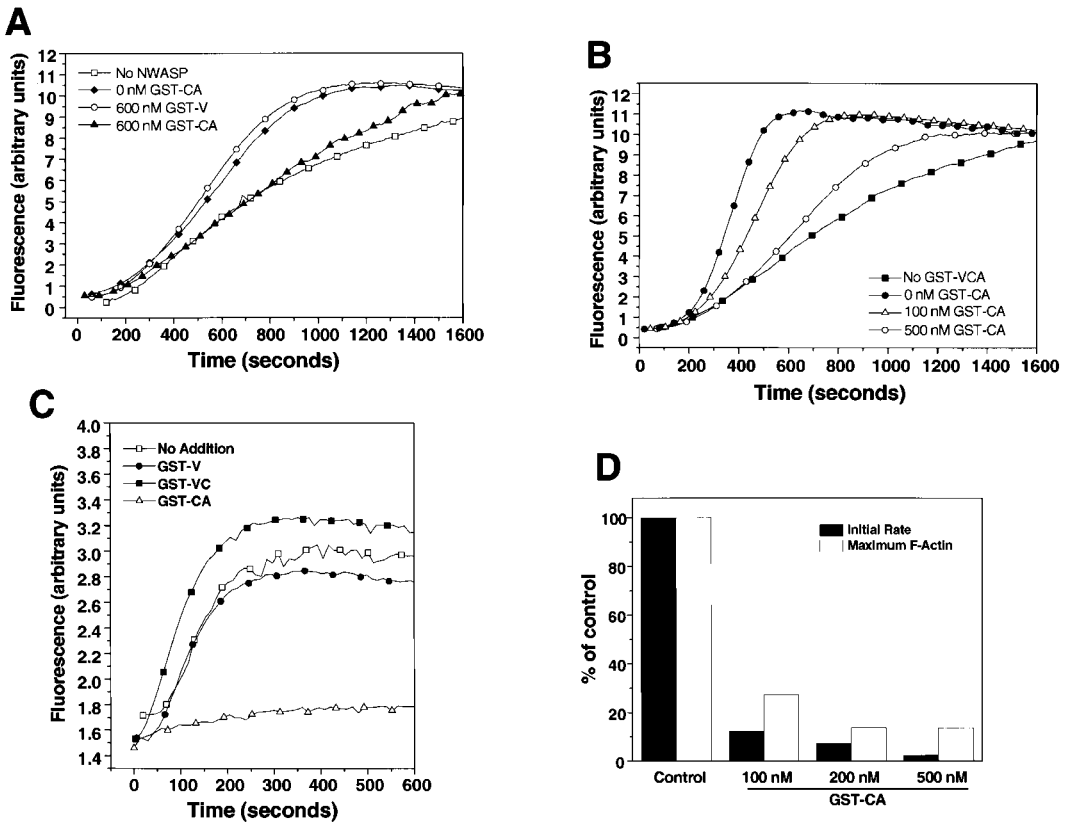

Figure 4. The GST-CA Fragment Can Inhibit the Interaction between N-WASP and the Arp2/3 Complex

(A) Stimulation of actin polymerization (2.5 μM actin and 60 nM Arp2/3 complex) by N-WASP (200 nM) is inhibited by GST-CA but not GST-V.

(B) Stimulation of actin polymerization (2.5 μM actin and 60 nM Arp2/3 complex) by GST-VCA (1 nM) is inhibited by GST-CA in a dose-dependent manner.

(C) Cdc42-stimulated actin polymerization in *Xenopus* HSS is inhibited by GST-CA, but not GST-V or GST-VC (200 nM each).

(D) Dose-dependent inhibition of Cdc42-stimulated actin polymerization in *Xenopus* HSS by GST-CA as compared using the initial rate and maximal level of F-actin assembly. The control depicts assembly in the absence of any GST-CA.

protein to accelerate actin polymerization. When the purified fragments were mixed with pure Arp2/3 complex, only the GST-VCA fusion protein accelerated assembly kinetics, shortening the lag phase and increasing the elongation rate by 30-fold (Figure 3C). Figure 3D clearly shows that the GST-VCA fragment shortens the lag phase to polymerization in a dose-dependent manner, suggesting that it can lower the kinetic barrier to nucleation. These effects are dependent on the presence of the Arp2/3 complex and can be inhibited by cytochalasin D (data not shown). The GST-V, GST-VC, and GST-CA fragments have no effect, even when used at 4-fold higher concentrations (Figure 3C). The GST-VCA fragment is both much more potent and effective in stimulating actin polymerization when compared to the full-length N-WASP, a point we will return to later.

Thus, the requirements for binding to the Arp2/3 complex are different from the requirements for activation, as summarized in Figure 3E.

A C-Terminal Fragment of N-WASP Can Act as a Dominant Inhibitor and Block the Function of N-WASP and the Arp2/3 Complex

The observation that the GST-CA fragment can bind to the Arp2/3 complex but cannot activate it suggests that it can be used as a competitive inhibitor to block the N-WASP–Arp2/3 interaction (Figure 3E). When this model was tested using purified components, GST-CA (but not GST-V, GST-VC, or GST) inhibits the ability of both full-length N-WASP and the GST-VCA fragment to stimulate actin polymerization in the presence of the Arp2/3 complex (Figures 4A and 4B).

The efficacy of the GST-CA fragment as a dominant negative was tested in *Xenopus* HSS for its effects on Cdc42-induced actin assembly. When used in extracts at concentrations roughly equivalent to the estimated endogenous Arp2/3 concentration (~100–300 nM), GST-CA specifically inhibited Cdc42-induced actin assembly (Figures 4C and 4D). This result strongly suggests that the kind of interaction between N-WASP and the Arp2/3 complex that we have observed using purified components in vitro is also required for Cdc42-induced actin polymerization in a more complete and physiological system.

The C-Terminal Domain of N-WASP Is at Least 100-Fold More Potent Than the Full-Length Protein

Using purified components, N-WASP (200 nM) can stimulate actin polymerization in the presence of only the Arp2/3 complex and G-actin (Figure 2). However, when added to *Xenopus* HSS at concentrations (400 nM) as

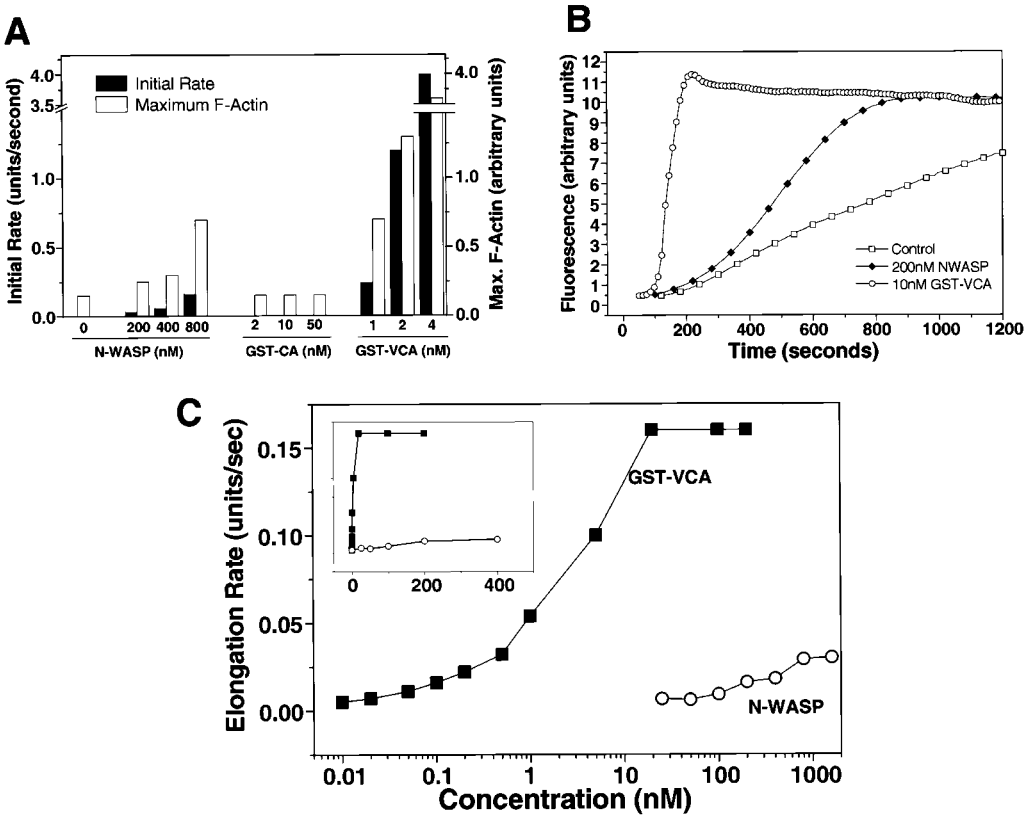

Figure 5. Full-Length N-WASP and the GST-VCA Fragment Activate Actin Polymerization with Different Potencies

(A) Comparion of spontaneous (Cdc42-independent) actin polymerization in *Xenopus* HSS treated with the indicated concentrations of full-length N-WASP, GST-CA, or GST-VCA.

(B) Actin polymerization (2.5 μM actin and 60 nM Arp2/3 complex) stimulated by full-length N-WASP (200 nM) or GST-VCA (10 nM).

(C) Dose–response curves showing the variation in the maximum rate of filament elongation as a function of increasing concentrations of either GST-VCA or full-length N-WASP in the presence of 60 nM Arp2/3 complex. The elongation rate was calculated from the linear phase of polymerization curves of the type shown in (B). The main graph depicts the concentrations (abscissa) on a log scale, whereas the inset depicts them on a linear scale. At higher concentrations of GST-VCA, the elongation rate saturates and is no longer a good indicator of activity. Instead, the shortening of the lag phase becomes more dramatic (Figure 3D).

high as 8-fold above the estimated endogenous N-WASP concentration (50 nM), full-length N-WASP did not stimulate spontaneous actin assembly in the absence of activated Cdc42 (Figure 5A). To test whether this difference in the behavior of N-WASP in the purified system compared to the extract is due to inhibitory factors that interact with its N terminus, we added the GST-VCA fragment to *Xenopus* HSS. We reasoned that GST-VCA would bypass the Cdc42 requirement and act in a dominant active fashion in the extract. Indeed, when GST-VCA was added to the HSS (in the absence of any activated Cdc42) even at very low concentrations, actin polymerization was dramatically stimulated: the effect of 1 nM GST-VCA was comparable to that of 800 nM N-WASP (Figure 5A). This observation suggests that N-WASP is regulated in extracts, a property that is conferred by the N terminus of the molecule.

How might the activity of N-WASP be regulated? It has been proposed that N-WASP is intrinsically inhibited and is activated when the VCA region is unmasked, perhaps by the binding of upstream regulators to the N terminus (Miki et al., 1998a). This model predicts a large difference between the full-length protein and the GST-VCA fragment in their ability to stimulate actin polymerization in the presence of the Arp2/3 complex. When full-length N-WASP was directly compared to the GST-VCA fragment, a large difference in activity was observed: 10 nM GST-VCA stimulates polymerization in vitro far more effectively than 200 nM N-WASP (Figure 5B).

To obtain a more quantitative measure of the activity difference between full-length N-WASP and the GST-VCA fragment, we generated dose–response curves for both proteins, using elongation rates as an indicator of activation (Figure 5C). The concentration required for half maximal activation is ~250 nM for the full-length protein and ~2 nM for GST-VCA (Figure 5C). Based on elongation rates, the C-terminal VCA domain is at least 100 times more potent than full-length N-WASP. This potency difference is also demonstrated by the ~20-fold higher molar ratio of GST-CA needed to inhibit GST-VCA compared to the full-length protein (Figures 4A and 4B). The efficacy of GST-VCA at inducing actin polymerization is also about 5-fold higher than that of N-WASP (Figure 5C). The difference in activity between GST-VCA

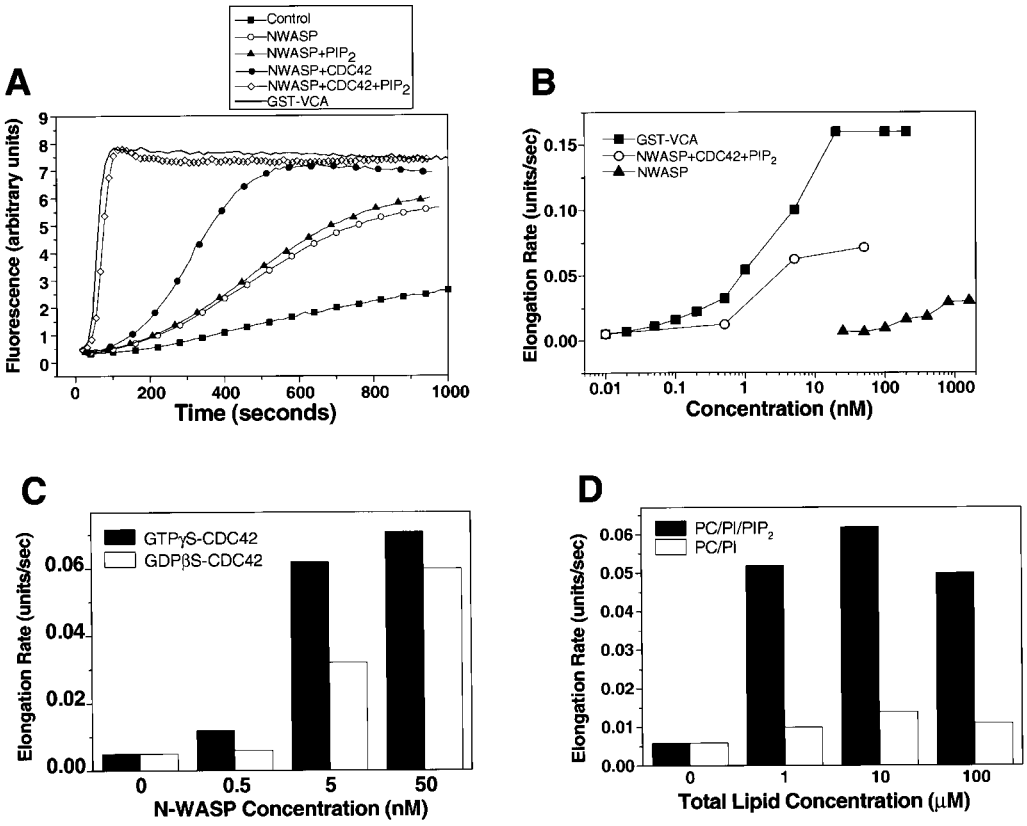

Figure 6. Cdc42 and PI(4,5)P_2 Coordinately Activate Full-Length N-WASP In Vitro

(A) The effect of GTPγS-Cdc42 (500 nM), PI(4,5)P_2-containing vesicles (100 μM, PC:PI:PI(4,5)P_2, 48:48:4), or both on actin polymerization (2.5 μM actin and 60 nM Arp2/3 complex) stimulated by N-WASP (200 nM). The solid line shows stimulation of actin polymerization under the same conditions by GST-VCA (200 nM) alone.

(B) Dose–response curves showing the maximum elongation rate of actin polymerization (2.5 μM actin and 60 nM Arp2/3 complex) as a function of the following molecules added: GST-VCA, full-length N-WASP, and full-length N-WASP stimulated with GTPγS-Cdc42 (50 nM) and PI(4,5)P_2-containing vesicles (100 μM, PC:PI:PI(4,5)P_2, 48:48:4). Note that the curve of N-WASP activated by PI(4,5)P_2 and GTPγS-Cdc42 starts to taper off between 8 and 80 nM because the Cdc42 is at a relatively low concentration in the experiment (50 nM); addition of higher concentrations of Cdc42 will drive activation to higher levels approaching those of GST-VCA (Figure 6A).

(C) Effects of Cdc42 bound to different nucleotides on N-WASP. Actin polymerization (2.5 μM actin and 60 nM Arp2/3 complex) was stimulated by N-WASP at the indicated concentrations in the presence of Cdc42 (50 nM, GTPγS or GDPβS charged) and PI(4,5)P_2-containing vesicles (10 μM, PC:PI:PI(4,5)P_2,48:48:4).

(D) Actin polymerization (2.5 μM actin and 60 nM Arp2/3 complex) was stimulated by N-WASP (5 nM) in the presence of Cdc42 (50 nM, GTPγS charged) and the indicated concentrations of lipid vesicles containing PC/PI (50:50) or PC/PI/PI(4,5)P_2 (48:48:4).

and full-length N-WASP is not due to the presence of the GST domain fused to VCA. In the presence of 60 nM Arp2/3 and 2.5 μM actin, 50 nM GST-VCA and 50 nM VCA (when cleaved from the GST moiety) stimulated the elongation rate by 35-fold and 25-fold, respectively, compared to the 2.5-fold stimulation obtained with a 4-fold higher concentration (200 nM) of full-length N-WASP.

Cdc42 and Phosphatidylinositol (4,5) Bisphosphate Can Synergistically Activate N-WASP In Vitro

The above data strongly support the hypothesis that full-length N-WASP is inhibited both in vitro and in *Xenopus* extracts (Miki et al., 1998a). To identify potential upstream regulators that may activate N-WASP in vitro, we focused on Cdc42 and PI(4,5)P_2, which have been implicated in actin assembly in *Xenopus* extracts (Ma et al., 1998a). Cdc42 and PI(4,5)P_2 interact with the GBD and PH domains of N-WASP, respectively (Figure 1A). Both domains are necessary for N-WASP to induce actin reorganization in fibroblasts (Miki et al., 1996, 1998a).

Addition of GTPγS-charged Cdc42 had only a small effect on the activity of full-length N-WASP, increasing the elongation rate by ~2-fold and having no effect on the duration of the lag phase (Figure 6A). Likewise, lipid vesicles containing phosphatidylcholine (PC), phosphatidylinositol (PI), and PI(4,5)P_2 in a 48:48:4 ratio failed to activate N-WASP (Figure 6A). However, the addition of both PI(4,5)P_2 and GTPγS-Cdc42 dramatically stimulated actin assembly (Figure 6A), an effect that depended on N-WASP and the Arp2/3 complex (data not shown). In fact, the ability of 200 nM N-WASP to activate actin assembly in the presence of PI(4,5)P_2 and GTPγS-Cdc42 was equal to that achieved by 200 nM GST-VCA (Figure 6A). To more precisely determine the activation potency of PI(4,5)P_2 and GTPγS-Cdc42, we compared

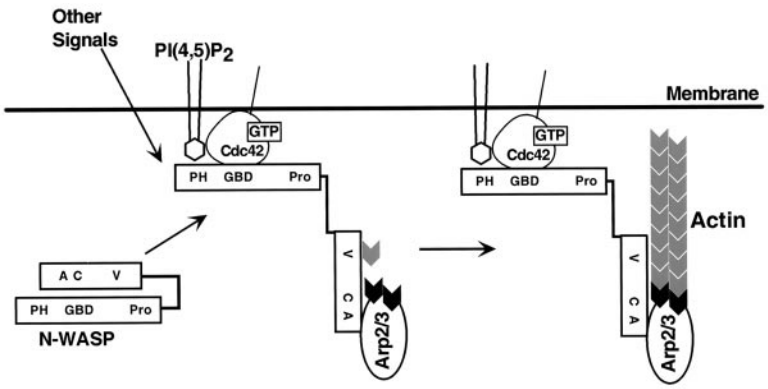

Figure 7. Signal-Dependent Actin Nucleation

A speculative model for the mechanism by which signals, such as Cdc42 and lipids, may regulate actin assembly at membrane-proximal sites by recruitment and activation of the Arp2/3 complex via N-WASP-like proteins.

the elongation rate as a function of the concentration of N-WASP, GST-VCA, or N-WASP activated by GTPγS-Cdc42 and $PI(4,5)P_2$ (Figure 6B). In the presence of Cdc42 and $PI(4,5)P_2$, the potency of N-WASP was increased to a level approaching that of GST-VCA, suggesting that N-WASP was fully activated by the two molecules.

The coordinate stimulation by Cdc42 and $PI(4,5)P_2$ favors GTPγS- over GDPβS-charged Cdc42, but it is not completely specific for the GTP form (Figure 6C). Selectivity is most apparent under conditions where the concentration of N-WASP is below that of Cdc42 (Figure 6C). At these low concentrations of N-WASP, the potency difference of GTPγS- over GDPβS-charged Cdc42 is ~5-fold. Since the PH domain of N-WASP has been reported to bind specifically to $PI(4,5)P_2$, we tested whether the stimulation seen above is specific for $PI(4,5)P_2$-containing vesicles (Miki et al., 1996). While control lipid vesicles containing only PC and PI (50:50) gave only an ~2-fold activation above the no lipid control, similar vesicles containing 4% $PI(4,5)P_2$ can activate by >10-fold (Figure 6D). Finally, GTPγS-charged Rho is ineffective at mediating stimulation (data not shown). Thus, the coordinate activation of N-WASP is Cdc42 and $PI(4,5)P_2$ specific and selective for the GTP form of Cdc42.

Discussion

The study of complex signal transduction networks comprising many direct and indirect pathways requires an integrated use of biochemical, genetic, and cell biological approaches. Biochemical reconstitution experiments can isolate the minimal set of components essential for biological function and help elucidate the detailed mechanism by which these components interact. Because small G proteins and phosphoinositides have many targets in the cell (Toker and Cantley, 1997; Van and D'Souza, 1997), the pathways that connect them to actin polymerization have been difficult to delineate. In this paper, we have demonstrated one such pathway in vitro, using both a cell-free system and purified components. We have shown that the Arp2/3 complex, required for actin nucleation in a variety of systems, is regulated by N-WASP. This interaction mediates Cdc42-induced actin polymerization in extracts and can be modulated by both $PI(4,5)P_2$ and Cdc42.

N-WASP and Actin Nucleation

Although N-WASP has been implicated in many actin-dependent processes, such as filopodium formation (Miki et al., 1998a) and the actin-based motility of *Shigella* (Suzuki et al., 1998), the mechanism by which it mediates actin polymerization has remained elusive. In this report, we provide evidence that N-WASP stimulates actin nucleation, a kinetically unfavored step of actin polymerization, by interacting with the Arp2/3 complex.

An N-WASP fragment consisting of the C-terminal 55 amino acids (CA region) directly binds to the Arp2/3 complex in vitro (Figure 3). This association is consistent with the observation that C-terminal segments of Scar1/WAVE and WASP, both of which share homology with the corresponding region in N-WASP, can bind to the Arp2/3 complex (Machesky and Insall, 1998). However, a longer segment of N-WASP, including both the Arp2/3-binding CA region and the actin-binding V region, is required for the activation of the Arp2/3 complex. The homologous VCA region of Scar1/WAVE has recently been shown to disrupt Arp2/3 localization and actin assembly at the cell periphery when overexpressed in Swiss 3T3 cells (Machesky and Insall, 1998). The authors also observed an increase in diffuse perinuclear phalloidin staining, consistent with our observation that the VCA region should both bind to and stimulate the Arp2/3 complex (Machesky and Insall, 1998). Disruption of peripheral actin assembly is likely to be a consequence of competition for the Arp2/3 complex or actin or both.

The *Listeria* protein ActA can dramatically stimulate the actin nucleation activity of the Arp2/3 complex, as evidenced by a shortening of the lag phase and an increase in the elongation rate (Welch et al., 1998). The VCA region of N-WASP has a very similar effect on actin polymerization kinetics in the presence of the Arp2/3 complex, suggesting that N-WASP-like proteins might be the cellular counterparts of ActA (Figures 2 and 3). Other than activation of nucleation, these kinetic changes in actin assembly could be produced by filament severing or an increased rate of elongation. We can essentially rule out both these alternative explanations because we failed to detect any significant severing activity or any change in the elongation rate of actin filaments in the presence of N-WASP, the Arp2/3 complex, or both (data not shown). Although ActA and N-WASP share no significant sequence homology, they do share a short

segment of similarity in the cofilin homology domain, which is also present in WASP, Scar1/WAVE, and Bee1 (Bi and Zigmond, 1999). The Δcof mutant, which is defective in Arp2/3 activation (Figure 2C), contains a four–amino acid deletion (Δ^{473}KRSK^{476}) within this segment.

How do N-WASP and the Arp2/3 complex act together to stimulate actin nucleation? Since the entire VCA domain of N-WASP is required for its ability to stimulate actin polymerization, we favor a model (Machesky and Insall, 1998) in which actin monomers and the Arp2/3 complex could be brought into proximity as a result of their interactions with the V and CA regions, respectively (Figure 7). In fact, the V domain is required for the ability of N-WASP to remodel the actin cytoskeleton when overexpressed in cells (Miki and Takenawa, 1998).

Cdc42 Signaling and the N-WASP–Arp2/3 Complex Interaction

Our results also shed light on the detailed mechanism by which Cdc42 regulates actin polymerization. We previously demonstrated a requirement for the Arp2/3 complex in Cdc42-induced actin assembly (Ma et al., 1998b). Here, we extend this work to show that N-WASP relays Cdc42 signals and directly activates the Arp2/3 complex in *Xenopus* extracts and in vitro with purified components. Most importantly, using purified N-WASP and purified Arp2/3 complex, we find that actin polymerization can be coordinately stimulated by Cdc42 and PI(4,5)P_2 (Figure 6).

This novel finding strongly suggests that the Cdc42 signaling pathway represents one cellular mechanism that stimulates actin polymerization by regulating the nucleation activity of the Arp2/3 complex (Ma et al., 1998b). The intracellular bacteria *Shigella* and *Listeria* appear to hijack the cellular machinery for actin assembly by intersecting this pathway at different points. The ActA protein of *Listeria* bypasses N-WASP and interacts with the Arp2/3 complex directly (Welch et al., 1998), whereas the VirG protein of *Shigella* functions by recruiting N-WASP (Suzuki et al., 1998). However, the Cdc42–N-WASP pathway probably represents only one of several cellular mechanisms that control actin assembly via the Arp2/3 complex. N-WASP belongs to a family of proteins, including WASP, Scar1/WAVE (Bear et al., 1998; Miki et al., 1998b), and Bee1 (Li, 1997), which share sequence homology at their C termini. Since the N termini of these proteins are quite different (Scar1/WAVE and Bee1 do not have the GBD or PH domains), they may transduce diverse upstream signals to a common effector, the Arp2/3 complex, through their homologous C termini. More generally, our results firmly establish that de novo actin nucleation is a step at which signaling pathways can regulate the actin cytoskeleton.

Signal-Dependent Actin Polymerization In Vitro

The difference in potency between the full-length N-WASP and its C-terminal VCA fragment both in vitro and in extracts suggests that N-WASP's activity is suppressed by 2–3 orders of magnitude. However, using purified components, we can maximally activate full-length N-WASP in the presence of two signaling molecules, Cdc42 and PI(4,5)P_2, that have previously been shown to interact with the GBD and PH domains in N-WASP (Miki et al., 1996). We have previously demonstrated that both Cdc42 and PI(4,5)P_2 can stimulate actin polymerization in *Xenopus* egg extracts (Ma et al., 1998a). Our in vitro data suggests that PI(4,5)P_2 may play an important role in N-WASP activation.

How is N-WASP regulated by both Cdc42 and PI(4,5)P_2? Miki et al. have suggested that N-WASP is regulated by an allosteric mechanism (1998a). Full-length N-WASP may exist in two conformations that are in equilibrium: an inactive conformation, in which the VCA domain is masked, and an active one in which the VCA domain is exposed and able to interact with the Arp2/3 complex. At rest, N-WASP largely populates the inactive conformation. This is supported by two observations: (1) full-length N-WASP only modestly activates the Arp2/3 complex (in comparison to the isolated VCA fragment); and (2) the full-length protein does not bind to the Arp2/3 complex under conditions where the association between its VCA fragment and Arp2/3 is readily detectable. However, since full-length N-WASP is completely inactive when added to extracts, we believe that other *trans*-acting factors may further suppress even the modest activity we have observed with the purified protein in vitro. Indeed, the majority of N-WASP from bovine brain extracts is present in high molecular weight complexes (unpublished observation). In any case, binding of upstream regulators, such as Cdc42 and PI(4,5)P_2, to the N terminus would activate N-WASP by stabilizing the active conformation of the molecule (Figure 7). In addition to Cdc42 and PI(4,5)P_2, the N-WASP protein binds to calmodulin and to SH3 domain–containing proteins and may be regulated in other ways (Miki et al., 1996). Unmasked in this active conformation, the VCA domain would promote nucleation by recruiting Arp2/3 via its CA region and G-actin via its V region. These speculative models of N-WASP activation and filament nucleation (summarized in Figure 7) await rigorous testing using kinetic analysis as well as by higher resolution mutagenesis. However, the results presented here establish N-WASP and the Arp2/3 complex as a core for signal-regulated actin assembly.

Experimental Procedures

Preparation of *Xenopus* Egg Extracts and Phospholipid Vesicles

Xenopus HSS was prepared as described previously (Ma et al., 1998b). Phospholipid vesicles containing PC:PI (50:50) or PC:PI:PI(4,5)P_2 (48:48:4) were prepared as described previously (Ma et al., 1998a) with the following modifications. Chloroform-dissolved phospholipids (PC, PI from Avanti Polar Lipids [Alabaster, AL]; PI[4,5]P_2 from Calbiochem) were mixed in the appropriate ratios and dried under nitrogen. The dried lipid mixture was resuspended in lipid buffer (10 mM HEPES [pH 7.7], 100 mM NaCl, 5 mM EGTA, and 50 mM sucrose) to a final concentration of 10 mM and then extruded through a 100 nm pore polycarbonate filter (Avanti) using the Mini-Extruder.

Preparation of Recombinant Proteins

The GST-Cdc42 and GST-Rho fusion proteins were prepared and loaded with different nucleotides (GTPγS or GDPβS) while still bound to glutathione-Sepharose beads according to established procedures (Ma et al., 1998a). All excess unbound nucleotide was washed away, and the G proteins were eluted in 20 mM HEPES (pH 7.6), 5 mM $MgCl_2$, 100 mM NaCl, 0.1% sodium cholate, and 10 mM glutathione.

Recombinant forms of full-length rat N-WASP, the H208D mutant,

and the Δcof mutant (deletion of amino acids 473–476) were prepared according to a published protocol, with modifications (Miki et al., 1998a). Proteins were expressed in insect (Sf9) cells and purified sequentially over heparin, Q-Sepharose, and Superdex 200 columns. GST fusion proteins containing various C-terminal regions of bovine N-WASP (shown in Figure 3) were prepared as described previously (Miki et al., 1996). The VCA fragment was cleaved from GST-VCA on glutathione-Sepharose beads using Factor Xa (Pharmacia), and the Factor Xa was separated from VCA using Benzamidine Sepharose (Pharmacia).

All proteins were quantitated by the Bradford assay (Bio-Rad, Hercules, CA) or by scanning densitometry of Gelcode Blue (Coomassie G-250) stained gels, using BSA as a standard in both cases. Proteins were stored at concentrations ≥1 mg/ml at −80°C and thawed and diluted immediately before use.

Preparation and Purification of Antibodies

Affinity-purified peptide antibodies against Arp3 and p34ARC were kindly provided by Matt Welch (University of California, San Francisco, CA). The anti-actin monoclonal antibody was purchased from Amersham (Arlington Heights, IL) and the anti-Glutathione S-Transferase polyclonal antibody from Santa Cruz Biotech (Santa Cruz, CA).

Full-length, Sf9-expressed rat N-WASP purified according to the procedures given above was used to raise antisera in rabbits (Zymed Labs, South San Francisco, CA). The antibodies were affinity purified essentially as described (Harlow and Lane, 1988).

Anti-Arp2 serum was generated by injecting rabbits (Zymed) with a Maltose-binding protein (MBP) fusion of human Arp2, which was expressed in *E. coli* and purified on an amylose affinity column (New England Biolabs, Beverly, MA). The specificity of the antiserum was confirmed by its ability to recognize (when used for immunoblotting) the Arp2 subunit from the purified bovine Arp2/3 described below.

Purification of the Arp2/3 Complex from Bovine Brain Extracts

The Arp2/3 complex was purified from bovine brain extracts by modifying a previously described protocol for the purification of Arp2/3 from *Xenopus* egg extracts (Ma et al., 1998b). High-speed extracts from calf brain were sequentially fractionated on Butyl Sepharose, DEAE Sepharose, S Sepharose, Phenyl Sepharose, and Superdex 200 columns, and the Arp2/3 complex was followed by immunoblotting with anti-Arp3 or anti-p34ARC. The bovine complex runs as a symmetric peak at the expected (~200 kDa) molecular weight on a gel filtration column and contains all seven polypeptide subunits (Figure 2A). The identities of four of these polypeptides (Arp2, Arp3, p41-ARC, and p34-ARC) were confirmed by immunoblotting. The bovine complex is also functional because it can support Cdc42-induced actin assembly when substituted for a *Xenopus* Arp2/3-containing fraction (Ma et al., 1998b).

Immunodepletion

For immunodepletion of N-WASP, high-speed supernatants of *Xenopus* egg extracts were mixed with affinity-purified anti-N-WASP antibodies at a concentration of 75 μg/ml and incubated on ice for 2 hr. The immune complexes were captured by adding one-tenth volume of packed protein-A Affiprep beads (Bio-Rad) and gently rocking at 4°C for 2 hr. Mock depletions were performed in the same way except that antibody buffer (PBS+40% glycerol) was used instead of the anti-N-WASP. The efficacy of the depletion was confirmed to be ≥95% by immunoblotting with the anti-N-WASP antibody.

Binding Assays

GST pull-down assays were performed by immobilizing equal amounts of the GST fusion proteins on glutathione-Sepharose beads (Pharmacia) at a concentration of approximately 5 mg/ml packed beads. For the Arp2/3 complex pull downs, ~5 μl of beads were incubated with 200 μl of bovine Arp2/3 complex (0.8 μM) in XB (10 mM HEPES [pH 7.6], 100 mM KCl, 1 mM $MgCl_2$, 0.1 mM EDTA, 1 mM DTT) plus 0.1% (v/v) Tween-20, 0.2 mM ATP, and 0.5 mg/ml chicken albumin (binding buffer). After gently rocking for ~1 hr at 4°C, the beads were washed two times in 100 μl of XB plus 0.1% (v/v) Tween-20 and 0.2 mM ATP. Proteins bound to the beads were eluted with SDS sample buffer. G-actin pull downs were performed in the same manner except that G-actin was used at a concentration of 0.05 μM, below the barbed end critical concentration.

Actin Polymerization Assays

Pyrene actin was used to follow actin polymerization in *Xenopus* extracts as described previously (Ma et al., 1998b). Polymerization was initiated by adding GTPγS-charged GST-Cdc42 at a concentration of 250 nM (unless otherwise noted).

To follow actin polymerization using purified components, pyrene G-actin or unlabeled G-actin was isolated by incubating freshly thawed proteins in G buffer (5 mM Tris-HCl [pH 8.0], 0.2 mM $CaCl_2$, 0.2 mM ATP, 0.2 mM DTT) for ~10 hr at 4°C and then removing residual F-actin by centrifugation at 400,000 × g for 1 hr. Polymerization reactions contained 1.5 μM unlabeled actin, 1 μM pyrene actin (50% labeled), 0.2 mM ATP, and various proteins in 80 μl of XB. All reaction components except the actin were first mixed together in XB and preincubated for 5 min. The reaction was started by adding a mixture of actin and pyrene actin to the preincubated protein mix, and fluorescence changes were measured in a fluorometer. In all the curves shown in the figures, actin polymerization was initiated at time = 0; the curves are shifted along the abscissa to account for the delay time between the addition of actin and the first fluorescence reading.

The curves shown in Figure 2B indicate an increase in the steady-state pyrene fluorescence in the presence of both Arp2/3 and N-WASP. This is not due to a change in filaments mass at steady state because the addition of phalloidin after the steady state is reached did not change the signal (data not shown). In cases where a clear steady state was attained, steady-state signals have been normalized to avoid underestimating the slopes of the control curves.

Data Analysis

All kinetic analyses were performed using either the software provided with the fluorescence spectrometer (SLM-Aminco) or using Origin (Microcal Software, Northampton, MA). Maximum elongation rates from the polymerization curves using the purified system have been calculated by performing a linear regression on the linear, elongation phase of the actin assembly curve. For pyrene assays in extracts, the initial rate and the maximum F-actin were calculated as described previously (Ma et al., 1998a). In all the curves shown in the figures, solid lines are drawn through all the data points collected; a symbol is only placed on every fifth or tenth point for clarity. All data shown in the figures were taken from experiments performed at least twice. When normalized to controls, data varied by ≤20% between independent experiments.

Acknowledgments

We thank Jeff Peterson for his help in the purification of the Arp2/3 complex from bovine brain extracts and for his preparation of lipid vesicles. We thank Teresita Bernal, Louise Evans, and Ann Georgi for their help in expressing recombinant proteins in Sf9 cells. We thank Tim Mitchison and Phil Allen for many helpful discussions and Matt Welch for providing antibodies against Arp3 and p34ARC. We also thank Jeff Peterson, Susannah Rankin, and Todd Stukenberg for comments on the manuscript. R. R. is a member of the Medical Scientist Training Program at Harvard Medical School. This work was supported in part by grants from the National Institutes of Health to M. W. K. (GM26875) and T. K. (5PO1 HL 59561-02).

Received February 25, 1999; revised March 24, 1999.

References

Arber, S., Barbayannis, F.A., Hanser, H., Schneider, C., Stanyon, C.A., Bernard, O., and Caroni, P. (1998). Regulation of actin dynamics through phosphorylation of cofilin by LIM-kinase. Nature *393*, 805–809.

Bear, J.E., Rawls, J.F., and Saxe, C.L., III (1998). SCAR, a WASP-related protein, isolated as a suppressor of receptor defects in late *Dictyostelium* development. J. Cell Biol. *142*, 1325–1335.

Beckerle, M.C. (1998). Spatial control of actin filament assembly: lessons from *Listeria*. Cell *95*, 741–748.

Bi, E., and Zigmond, S.H. (1999). Where the WASP stings. Curr. Biol. *9*, R160–R163.

Drubin, D.G., and Nelson, W.J. (1996). Origins of cell polarity. Cell *84*, 335–344.

Field, C., Li, R., and Oegema, K. (1999). Cytokinesis in eukaryotes: a mechanistic comparison. Curr. Opin. Cell Biol. *11*, 68–80.

Fukuoka, M., Miki, H., and Takenawa, T. (1997). Identification of N-WASP homologs in human and rat brain. Gene *196*, 43–48.

Hall, A. (1998). Rho GTPases and the actin cytoskeleton. Science *279*, 509–514.

Harlow, E., and Lane, D. (1988). Antibodies: A Laboratory Manual (Cold Spring Harbor, NY: Cold Spring Harbor Press), pp. 283–318.

Hartwig, J.H., Bokoch, G.M., Carpenter, C.L., Janmey, P.A., Taylor, L.A., Toker, A., and Stossel, T.P. (1995). Thrombin receptor ligation and activated Rac uncap actin filament barbed ends through phosphoinositide synthesis in permeabilized human platelets. Cell *82*, 643–653.

Johnson, D.I. (1999). Cdc42: an essential Rho-type GTPase controlling eukaryotic cell polarity. Microbiol. Mol. Biol. Rev. *63*, 54–105.

Kelleher, J.F., Atkinson, S.J., and Pollard, T.D. (1995). Sequences, structural models, and cellular localization of the actin-related proteins Arp2 and Arp3 from *Acanthamoeba*. J. Cell Biol. *131*, 385–397.

Li, R. (1997). Bee1, a yeast protein with homology to Wiscott-Aldrich syndrome protein, is critical for the assembly of cortical actin cytoskeleton. J. Cell Biol. *136*, 649–658.

Ma, L., Cantley, L.C., Janmey, P.A., and Kirschner, M.W. (1998a). Corequirement of specific phosphoinositides and small GTP-binding protein Cdc42 in inducing actin assembly in *Xenopus* egg extracts. J. Cell Biol. *140*, 1125–1136.

Ma, L., Rohatgi, R., and Kirschner, M.W. (1998b). The Arp2/3 complex mediates actin polymerization induced by the small GTP-binding protein Cdc42. Proc. Natl. Acad. Sci. USA *95*, 15362–15367.

Machesky, L.M., and Gould, K.L. (1999). The Arp2/3 complex: a multifunctional actin organizer. Curr. Opin. Cell Biol. *11*, 117–121.

Machesky, L.M., and Insall, R.H. (1998). Scar1 and the related Wiskott-Aldrich syndrome protein, WASP, regulate the actin cytoskeleton through the Arp2/3 complex. Curr. Biol. *8*, 1347–1356.

Machesky, L.M., Atkinson, S.J., Ampe, C., Vandekerckhove, J., and Pollard, T.D. (1994). Purification of a cortical complex containing two unconventional actins from *Acanthamoeba* by affinity chromatography on profilin-agarose. J. Cell Biol. *127*, 107–115.

Miki, H., and Takenawa, T. (1998). Direct binding of the verprolin-homology domain in N-WASP to actin is essential for cytoskeletal reorganization. Biochem. Biophys. Res. Commun. *243*, 73–78.

Miki, H., Miura, K., and Takenawa, T. (1996). N-WASP, a novel actin-depolymerizing protein, regulates the cortical cytoskeletal rearrangement in a PIP2-dependent manner downstream of tyrosine kinases. EMBO J. *15*, 5326–5335.

Miki, H., Sasaki, T., Takai, Y., and Takenawa, T. (1998a). Induction of filopodium formation by a WASP-related actin-depolymerizing protein N-WASP. Nature *391*, 93–96.

Miki, H., Suetsugu, S., and Takenawa, T. (1998b). WAVE, a novel WASP-family protein involved in actin reorganization induced by Rac. EMBO J. *17*, 6932–6941.

Mitchison, T.J., and Cramer, L.P. (1996). Actin-based cell motility and cell locomotion. Cell *84*, 371–379.

Mullins, R.D., Heuser, J.A., and Pollard, T.D. (1998). The interaction of Arp2/3 complex with actin: nucleation, high affinity pointed end capping, and formation of branching networks of filaments. Proc. Natl. Acad. Sci. USA *95*, 6181–6186.

Nobes, C.D., Hawkins, P., Stephens, L., and Hall, A. (1995). Activation of the small GTP-binding proteins rho and rac by growth factor receptors. J. Cell Sci. *108*, 225–233.

Ridley, A.J., and Hall, A. (1992). The small GTP-binding protein rho regulates the assembly of focal adhesions and actin stress fibers in response to growth factors. Cell *70*, 389–399.

Ridley, A.J., Paterson, H.F., Johnston, C.L., Diekmann, D., and Hall, A. (1992). The small GTP-binding protein rac regulates growth factor-induced membrane ruffling. Cell *70*, 401–410.

Suzuki, T., Miki, H., Takenawa, T., and Sasakawa, C. (1998). Neural Wiskott-Aldrich syndrome protein is implicated in the actin-based motility of *Shigella flexneri*. EMBO J. *17*, 2767–2776.

Symons, M., Derry, J.M., Karlak, B., Jiang, S., Lemahieu, V., Mccormick, F., Francke, U., and Abo, A. (1996). Wiskott-Aldrich syndrome protein, a novel effector for the GTPase CDC42Hs, is implicated in actin polymerization. Cell *84*, 723–734.

Toker, A., and Cantley, L.C. (1997). Signalling through the lipid products of phosphoinositide-3-OH kinase. Nature *387*, 673–676.

Van, A.L., and D'Souza, S.C. (1997). Rho GTPases and signaling networks. Genes Dev. *11*, 2295–2322.

Welch, M.D., DePace, A.H., Verma, S., Iwamatsu, A., and Mitchison, T.J. (1997a). The human Arp2/3 complex is composed of evolutionarily conserved subunits and is localized to cellular regions of dynamic actin filament assembly. J. Cell Biol. *138*, 375–384.

Welch, M.D., Iwamatsu, A., and Mitchison, T.J. (1997b). Actin polymerization is induced by Arp2/3 protein complex at the surface of *Listeria monocytogenes*. Nature *385*, 265–269.

Welch, M.D., Rosenblatt, J., Skoble, J., Portnoy, D.A., and Mitchison, T.J. (1998). Interaction of human Arp2/3 complex and the *Listeria monocytogenes* ActA protein in actin filament nucleation. Science *281*, 105–108.

Winter, D., Podtelejnikov, A.V., Mann, M., and Li, R. (1997). The complex containing actin-related proteins Arp2 and Arp3 is required for the motility and integrity of yeast actin patches. Curr. Biol. *7*, 519–529.

Yang, N., Higuchi, O., Ohashi, K., Nagata, K., Wada, A., Kangawa, K., Nishida, E., and Mizuno, K. (1998). Cofilin phosphorylation by LIM-kinase 1 and its role in Rac-mediated actin reorganization. Nature *393*, 809–812.

Zigmond, S.H. (1998). Actin cytoskeleton: the Arp2/3 complex gets to the point. Curr. Biol. *8*, R654–R657.